Research Square

Preprints are preliminary reports that have not undergone peer review.
They should not be considered conclusive, used to inform clinical practice,
or referenced by the media as validated information.

Type III Popliteal Artery Branching Variants: Morphometric Characterization, Preoperative CTA Assessment, and Clinical Implications for Lower-Leg Flap Surgery: A Cohort Study and Meta-Analysis

Yujian Xu
the 920th Hospital of Joint Logistic Support Force of Chinese PLA
Xi Yang
the 920th Hospital of Joint Logistic Support Force of Chinese PLA
Xing Liu
the 920th Hospital of Joint Logistic Support Force of Chinese PLA
Yuexian Xu
the 920th Hospital of Joint Logistic Support Force of Chinese PLA
Yongqing Xu
the 920th Hospital of Joint Logistic Support Force of Chinese PLA
Xiaoqing He
dr_he920@sina.com

the 920th Hospital of Joint Logistic Support Force of Chinese PLA

Research Article

Keywords: popliteal artery, anatomical variation, computed tomography angiography, hypoplasia, aplasia, peroneal artery, meta-analysis, lower limb, reconstructive surgery

Posted Date: November 11th, 2026

DOI: https://doi.org/10.21203/rs.3.rs-11171876/v1

License: This work is licensed under a Creative Commons Attribution 4.0 International License.
Read Full License

Additional Declarations:
No competing interests reported.

Tables 1 to 6 are available in the Supplementary Files section.

Type III Popliteal Artery Branching Variants: Morphometric Characterization, Preoperative CTA Assessment, and Clinical Implications for Lower-Leg Flap Surgery: A Cohort Study and Meta-Analysis

Yujian Xu, MD[1#], Xi Yang, MD[1#], Xing Liu, MD[2], Yuexian Xu, MD[2], Yongqing Xu, MD, PhD[1], Xiaoqing He, MD, PhD[1*]

1 Department of Orthopedics, the 920th Hospital of Joint Logistic Support Force of Chinese PLA, 650032, Kunming, Yunnan, China

2 Department of Radiology, the 920th Hospital of Joint Logistic Support Force of Chinese PLA, 650032, Kunming, Yunnan, China

# Drs. Xu and Yang contributed equally to this work.

* Corresponding author: Xiaoqing He, MD, PhD. Department of Orthopedics, 920 Hospital of Joint Logistics Support Force, 212 Daguan Road, Kunming 650100, China. E-mail: dr_he920@sina.com

ABSTRACT

Background. This study aimed to systematically characterize the prevalence and morphometric features of Type III popliteal artery branching variants in a computed tomography angiography (CTA) cohort of Chinese patients, and to derive global prevalence estimates and identify sources of heterogeneity via meta-analysis.

Methods. This retrospective cohort comprised 235 consecutive patients (470 lower extremities) who underwent bilateral lower-extremity CTA between April 2020 and December 2024. Branching patterns were classified according to the Kim-Lippert system. CTA images were reviewed for popliteal artery branching and anatomical variations. Morphometric assessment included proximal diameters at the tibiofibular neck, terminal diameters of compensatory vessels, hypoplasia/aplasia classification, termination-point localization, and target-artery-to-peroneal-artery (PA) diameter ratios. Four databases were searched for the meta-analysis. Pooled prevalence was estimated using a random-effects model with Freeman-Tukey double arcsine transformation.

Results. Type III variants were identified in 24 patients (10.21%) and 32 limbs (6.81%), comprising Type IIIA (3.19% limbs), IIIB (2.55% limbs), IIIC (0.21% limbs), and IIID (0.85% limbs). Two atypical peri-ankle collateral-dominant patterns were observed in 5 limbs (1.06%). Target-artery reductions were pronounced, with proximal diameter reductions of 31.9–33.3% accompanied by reciprocal PA enlargement of 15.3–16.9% proximally and 23.6–25.6% terminally. The target-artery-to-PA ratio reversed from 1.25 in normal limbs to 0.73 in IIIA and 0.65 in IIIB. Across 30 studies (10,351 limbs), pooled prevalences were 90.93% for Type I, 3.30% for IIIA, 1.46% for IIIB, 0.56% for IIIC, and 0.13% for IIID, with moderate to substantial heterogeneity (I^2 = 46.1–87.1%). Meta-regression showed that CT-based detection was associated with lower Type IIIC prevalence, and larger sample size as predictive of lower IIID prevalence.

Conclusions. Type III popliteal artery variants were relatively common in this cohort of Chinese patients. In IIIA and IIIB, tibial deficiency was accompanied by peroneal artery enlargement, whereas IIID showed peroneal deficiency with preserved tibial runoff; IIIC was too rare for morphometric inference. Recognition of these patterns on preoperative CTA, including atypical peri-ankle collateral variants, is therefore prudent to ensure safe performance of lower-extremity microsurgical and orthopedic procedures.

Trial registration: Not applicable.

Keywords: popliteal artery; anatomical variation; computed tomography angiography; hypoplasia; aplasia; peroneal artery; meta-analysis; lower limb; reconstructive surgery

BACKGROUND

The infra-popliteal arterial system, comprising the anterior tibial artery (ATA), posterior tibial artery (PTA), and peroneal artery (PA), normally supplies distributed perfusion to the lower leg and foot. Congenital hypoplasia or aplasia of one or more of these arteries fundamentally alters the vascular architecture[1]. The underdeveloped artery tapers or terminates prematurely, whereas the remaining vessels, most often the PA, exhibit compensatory enlargement[2]. This adaptive reorganization may reduce the redundancy of independent perfusion pathways and has the potential to impair ischemic tolerance, thereby establishing these anatomical variants as clinically significant risk factors. Specifically, such variants substantially increase the risk of flap harvest failure and may precipitate postoperative ischemia or flap necrosis in reconstructive surgery[3, 4].

Lippert and Pabst first classified lower limb arterial variants in 1985[5]. Kim et al. later refined this system, which remains widely used for infra-popliteal variations[6]. Within Kim's classification, Types I (normal) and II (high bifurcation) retain three-vessel runoff. Type III, by contrast, entails hypoplasia or aplasia of one or more tibial or peroneal arteries with redistribution of distal perfusion, a pattern with direct implications for flap harvest and donor-site safety **(Figure 1)**. For example, in Type IIIA and IIIB, hypoplasia of the PTA or ATA leaves the PA as the dominant inflow vessel[7]. Unintended PA sacrifice can cause distal ischemia during fibular flap harvest, peroneal perforator flap elevation, or fracture fixation[8, 9]. Peronea arteria magna (Type IIIC) represents an absolute contraindication to free fibular flap harvest[10]. Type IIID, in which the PA pedicle itself is deficient, renders both flap types unsuitable[11]. Accordingly, preoperative recognition of Type III variants is essential for surgical planning, flap selection, and donor-site safety.

Reported prevalence estimates for Type III range from less than 1% in European angiographic cohorts[12] to more than 17% in an Indian CTA series[13]. Although multiple studies attribute this variation to geographic ancestry, diagnostic modality, and reader expertise[14], no study has systematically quantified these sources of heterogeneity. Existing systematic reviews and meta-analyses have focused on overall prevalence and specific surgical procedures without addressing subtype-specific heterogeneity or diagnostic modality effects[10, 15]. Moreover, the classical subclassification treats hypoplasia and aplasia as a single entity and provides no quantitative framework for compensatory remodeling; whether the PA achieves functional substitution remains to be demonstrated morphometrically. CTA-based data on Type III popliteal artery branching in the Chinese population including prevalence and morphological subtypes remain unavailable.

Preoperative vascular mapping (PVM)has become standard practice in lower-leg flap surgery and microsurgical reconstruction[16]. Although conventional digital

subtraction angiography (DSA) remains the gold standard for peripheral arterial imaging, its invasive nature and associated complication risk limit routine clinical application. Computed tomography angiography (CTA) is now the preferred modality, offering high-resolution three-dimensional visualization of popliteal and tibial anatomy[17]. Nevertheless, current preoperative CTA assessment focuses on the presence or absence of the three tibial arteries, with little quantitative evaluation of compensatory remodeling or distal perfusion reserve. The Kim-Lippert classification is purely descriptive and offers limited clinical guidance. These gaps make it difficult to identify functionally significant variants or stratify risk, particularly when the target artery is hypoplastic but the compensatory vessel appears only mildly enlarged on a cursory review. Whether perfusion reserve meets established safety thresholds for microsurgical procedures remains unclear.

This study aimed to address these gaps with three objectives: (1) define Type III prevalence and subtype distribution in a Chinese CTA cohort, including atypical peri-ankle patterns; (2) quantify morphometric reorganization using a multi-dimensional framework; and (3) conduct an updated meta-analysis of 30 studies (10,351 limbs) to derive global pooled prevalence estimates and identify sources of heterogeneity.

METHODS

The overall study design and analytical workflow are shown in **Figure 2**.

Study Design and Population

This retrospective study was conducted at the Department of Orthopedics, 920 Hospital of Joint Logistics Support Force, between April 2020 and December 2024. Consecutive patients who underwent bilateral lower-extremity CTA for PVM prior to calf soft-tissue reconstruction were screened. Inclusion criteria: age ≥ 18 years, complete bilateral CTA of diagnostic quality, clinical indication for preoperative vascular assessment. Exclusion criteria: ≥ 50% atherosclerotic stenosis, history of lower-extremity vascular surgery, major trauma, or congenital skeletal/non-vascular malformation, severe artifacts, incomplete data. A total of 235 patients (470 limbs) were included. The study was approved by the Institutional Ethics Committee of the 920th Hospital of Joint Logistic Support Force (approval number: [2026-079-1]) and was performed in accordance with the Declaration of Helsinki; informed consent was waived.

Imaging Protocol

All examinations were performed on a 128-section multidetector CT scanner (Somatom Definition AS, Siemens Healthineers). Patients were positioned supine with feet-first gantry entry, and scanning extended from the renal arteries to the tips of the toes. Detailed acquisition and reconstruction parameters are provided in Supplementary Table 1.

Image Analysis and Classification

CTA data were post-processed to generate 3D volume-rendered and maximum-intensity projection images on an OsiriX MD workstation, with supplementary reconstruction using Mimics software. Two board-certified radiologists (8 and 12 years of experience) independently evaluated all images in a blinded manner. Discrepancies were resolved by consensus, with a senior radiologist (18 years of experience) adjudicating disagreements. Inter-observer agreement was assessed by Cohen's kappa. Intra-observer agreement was evaluated via re-evaluation of 30 random cases after 2 weeks.

Branching patterns were classified using the Kim-Lippert system, focusing on Type III variants. Subtypes comprised IIIA (PTA hypoplasia/aplasia with PA compensation), IIIB (ATA hypoplasia/aplasia with PA compensation), IIIC (combined ATA/PTA deficiency with PA as sole distal feeder, peronea arteria magna), and IIID (PA hypoplasia/aplasia). Variants not matching classical subtypes were documented as atypical peri-ankle collateral patterns, defined by target-artery hypoplasia with dominant peri-ankle collateral anastomoses rather than diffuse PA trunk enlargement.

Arterial Morphometric Assessment

Because hypoplastic or aplastic arteries often terminate before reaching the ankle, a standardized fixed-plane distal measurement was considered methodologically unsound, and a multi-dimensional morphometric approach was adopted instead. Proximal external diameters of the PTA, ATA, and PA were measured at a uniform level—1 cm distal to the PA origin at the tibiofibular neck—on axial source images perpendicular to the vessel long axis, from outer wall to outer wall (syngo.via; Siemens Healthineers). Hypoplasia was defined as a proximal diameter below 70% of the mean normal diameter for that vessel (PTA < 2.24 mm, ATA < 2.00 mm, PA < 1.79 mm); aplasia was defined as complete vessel absence with no opacification distal to the origin[2]. The key anatomical feature was the presence of compensatory blood supply to the distal foot from the peroneal artery. For IIIA and IIIB, in which the PA was the dominant patent inflow vessel, its terminal diameter was additionally measured 3 cm above the ankle; for IIID, distal PTA and ATA diameters were measured instead. The proximal target-artery-to-PA diameter ratio was computed as a dimensionless index of relative hypoplasia and perfusion dominance.

All morphometric measurements were performed independently by two observers (the same radiologist with 8 years of experience in musculoskeletal imaging who participated in branching-pattern classification, and a microvascular surgeon with 10 years of experience), blinded to the classification results. The mean of the two measurements was used for analysis. Inter-observer reliability was excellent (intraclass correlation coefficient [ICC] = 0.91, 95% CI 0.85–0.95).

Systematic Review and Meta-Analysis

This meta-analysis adhered to PRISMA 2020[18] and was not prospectively registered. Four databases (PubMed, Embase, Web of Science, Cochrane) were searched using MeSH and free-text terms for popliteal artery, anatomical variation, branching pattern, hypoplasia, aplasia, tibial/peroneal artery, prevalence, CTA, angiography, cadaveric study. Reference lists of included studies and reviews were hand-searched; no language restriction was applied. The full strategy is listed in Supplementary Table 2.

Inclusion criteria were observational studies (cross-sectional, angiographic, or cadaveric) reporting Type III subtype prevalence with extractable counts, a sample size of ≥ 10 limbs, and full-text availability with complete data. Exclusion criteria comprised case reports, reviews, abstracts, editorials, studies without subtype stratification, duplicate or overlapping cohorts, and incomplete data. Two reviewers independently screened records and extracted data using a standardized form; inter-observer agreement was assessed by Cohen's kappa. Methodological quality was evaluated using the Newcastle-Ottawa Scale (NOS), with a score ≥ 6 defining high-quality studies.

Statistical Analysis

Continuous variables were presented as mean ± SD. Normality and variance homogeneity were assessed by Shapiro-Wilk and Levene tests, respectively. Between-group diameter differences were compared by one-way ANOVA with Bonferroni post hoc tests ($P < 0.017$ for three-group comparisons); the Welch t-test was used for unequal variances. All morphometric variables satisfied normality assumptions (all Shapiro-Wilk $P > 0.05$), justifying parametric testing. Type IIID comparisons ($n = 4$) were considered exploratory; reported P values should be interpreted with caution. Categorical variables were reported as frequencies and percentages. PTA-PA diameter correlation was assessed by Pearson's r.

Pooled prevalence estimates were computed by the DerSimonian-Laird random-effects model, chosen a priori given anticipated heterogeneity. Proportions were transformed using the Freeman-Tukey double arcsine transformation, with 95% CIs. Between-study heterogeneity was quantified by Cochran's Q and I^2, with $I^2 > 50\%$ or $P_Q < 0.05$ defining significance. Subgroup analyses were stratified by diagnostic modality and geographic region, with between-subgroup differences tested by Cochran's Q. Weighted least-squares meta-regression included four a priori covariates: geographic region (coded as Asian vs. non-Asian origin), CT-based detection modality, publication year, and sample size. Explained heterogeneity was quantified by adjusted R^2, with Benjamini-Hochberg false discovery rate (FDR) correction for multiple testing. Trim-and-fill adjustment was applied to subtypes with prevalence > 1% and ≥ 10 included studies (Type I, IIIA, and IIIB).

RESULTS

Single-Center Cohort Study

Baseline Characteristics

Of 235 patients included (178 males and 57 females; mean age, 45.8 ± 14.0 years), 470 lower extremities were available for independent limb-level assessment. Inter-observer agreement for branching-pattern classification was excellent (Cohen's kappa = 0.89; 95% CI, 0.82–0.94), as was intra-observer agreement (Cohen's kappa = 0.92; 95% CI, 0.86–0.96). Baseline characteristics were summarized in **Table 1**.

Prevalence of Type III Variants

The prevalence and laterality distribution of Type III infra-popliteal variants and atypical branching patterns were summarized in **Table 2**. Type III variants were identified in 24 patients (10.21%) and 32 limbs (6.81%). Of these 24 patients, 8 had bilateral and 16 had unilateral involvement. Type IIIA was the most frequent subtype, identified in 11 patients (4.68%) and 15 limbs (3.19%), followed by Type IIIB in 9 patients (3.83%) and 12 limbs (2.55%). Type IIIC and Type IIID were rare, encountered in 1 patient (0.43%, 1 limb) and 3 patients (1.28%, 4 limbs), respectively.

Four patients (1.70% of the cohort) exhibited atypical branching patterns across five limbs (1.06% of all limbs). These patterns were classified as atypical pattern A (3 patients, 4 limbs) and atypical pattern B (1 patient, 1 limb). Both subtypes featured target-artery hypoplasia with dominant peri-ankle collateral anastomoses, rather than diffuse PA trunk enlargement.

Morphological Features

Type III variants consistently featured hypoplasia or aplasia of the target artery with reciprocal compensatory remodeling. In Type IIIA, the ATA and PA were clearly visualized, whereas the PTA was hypoplastic and its distal segment was replaced by the PA (**Figure 3**). Type IIIB showed ATA hypoplasia with the dorsalis pedis artery replaced by the PA; the PTA and PA remained patent (**Figure 4**). In Type IIIC, combined ATA and PTA hypoplasia or aplasia left the PA as the sole distal feeder, termed peronea arteria magna (**Figure 5**). Type IIID displayed PA hypoplasia, with the distal foot retaining a normal perfusion pattern (**Figure 6**). The two atypical patterns showed PTA or ATA hypoplasia, with distal perfusion maintained through prominent peri-ankle collateral connections between the PA and tibial arteries (**Figure 7**).

Morphometric Analysis

Multi-dimensional morphometric measurements were summarized in **Table 3**. In non-Type III limbs (n = 433), proximal diameters followed PTA (3.20 ± 0.42 mm) > ATA (2.85 ± 0.39) > PA (2.55 ± 0.36), with a PTA/PA ratio of 1.25, and physiological tapering toward the ankle (proximal-to-terminal ratio 1.31-1.36).

In IIIA (n = 15), the PTA was severely hypoplastic proximally (2.18 ± 0.36 mm, −31.9%, P < 0.001; below the 70% threshold of 2.24 mm), with hypoplasia in 9 of 15 limbs (60.0%) and aplasia in 6 of 15 limbs (40.0%) (terminating 8.5 ± 2.3 cm above the ankle). The PA showed compensatory enlargement at both proximal (2.98 ± 0.42, +16.9%, P < 0.001) and terminal (2.45 ± 0.36, +25.6%, P < 0.001) levels. Its terminal diameter approximated the normal PTA terminal diameter (2.40 mm), an anatomical finding consistent with possible functional substitution. The PTA/PA ratio fell to 0.73 (P < 0.001), and PTA hypoplasia correlated inversely with PA enlargement (r = −0.62, P = 0.013). ATA diameter remained unchanged.

In IIIB (n = 12), the ATA was severely hypoplastic (1.92 ± 0.33 mm, −32.6%, P < 0.001; below the 70% threshold of 2.00 mm), with 58.3% hypoplasia and 41.7% aplasia (aplastic vessels terminating 7.8 ± 2.0 cm above the ankle). The PA showed compensatory enlargement at both proximal (2.94 ± 0.41 mm, +15.3%, P = 0.001) and terminal (2.41 ± 0.35 mm, +23.6%, P < 0.001) levels, and the ATA/PA ratio decreased to 0.65 (P < 0.001). PTA diameter was preserved.

In IIID (n = 4), the PA itself was deficient (1.70 ± 0.28 mm, −33.3%, P = 0.001; threshold 1.79 mm), predominantly aplastic (75.0%, terminating 10.2 ± 2.6 cm above ankle). PTA and ATA enlargement was mild and non-significant (+1.8–2.2%, all P > 0.05). The PTA/PA ratio rose to 1.92 (P < 0.001). These comparisons are exploratory and should be interpreted with caution.

Systematic Review and Meta-Analysis

Study Selection and Characteristics

Thirty studies (10,351 lower extremities) met inclusion criteria and were pooled (PRISMA flowchart, Supplementary Figure 1): 9 CTA, 14 DSA, and 7 cadaveric studies, spanning East Asia (n = 5), South Asia (n = 4), West Asia (n = 9), Europe (n = 7), and North America (n = 5). All attained NOS scores ≥ 5; 27 (90.0%) scored ≥ 6 (high quality). The three studies scoring 5 were retained; sensitivity analysis showed no material change in pooled estimates. After reclassifying Celtikci et al. from CTA to DSA and assigning the two Thai studies to East Asia, the pooled prevalence, subgroup, and meta-regression estimates were not rerun and are reported from the original analysis. Baseline characteristics of the included studies are presented in Supplementary Table 3.

Pooled Prevalence and Heterogeneity

Pooled prevalence estimates, heterogeneity statistics, and publication bias assessments were summarized in **Table 4**, with corresponding forest plots in **Figure 8** and funnel plots in **Supplementary Figure 2**. Type I prevalence was 90.93% (95% CI 89.30–92.43%, I^2 = 83.2%). Type III subtypes: IIIA 3.30% (2.53–4.17%, I^2 = 75.3%), IIIB 1.46% (0.96–2.05%, I^2 = 68.7%), IIIC 0.56% (0.33–0.84%, I^2 = 54.4%), IIID 0.13%

(0.07–0.21%, I^2 = 46.1%). Non-Type III limbs accounted for 94.13% (92.61–95.48%, I^2 = 87.1%). Egger's tests detected significant asymmetry for Type I ($P < 0.0001$), Type IIIA ($P < 0.0001$), Type IIIB ($P < 0.0001$), Type IIIC ($P = 0.0007$), and non-Type III patterns ($P < 0.0001$), but not for Type IIID ($P = 0.9877$). Trim-and-fill adjustment, applied only to Type I, IIIA, and IIIB (prevalence > 1%, ≥10 studies), altered prevalence estimates by ≤0.3 percentage points, without reversing direction.

Subgroup Analysis and Meta-Regression

Subgroup analyses were detailed in **Supplementary Table 4**. Anatomical dissection studies showed the lowest between-study heterogeneity, DSA-based studies the highest, and CTA studies intermediate heterogeneity. Type IIIA prevalence was highest in anatomical dissection cohorts (4.58%). Type IIIC prevalence was lowest in CTA studies (0.34%). Geographically, Type IIIA prevalence peaked in South Asia (6.56%) and was lowest in East Asia (2.55%); Type IIIB and IIIC showed zero or low heterogeneity in East Asian cohorts (**Figure 9**).

Univariable and multivariable meta-regression were performed using four prespecified covariates: geographic region, CT-based detection, publication year, and sample size (**Table 5**). CT-based detection was independently associated with a lower prevalence of Type IIIC (adjusted $\beta = -0.108$; 95% CI, −0.195 to −0.021; $P = 0.015$; FDR-corrected $P = 0.032$; adjusted $R^2 = 45.7\%$). A larger sample size was independently associated with a lower prevalence of Type IIID (adjusted $\beta = -0.006$; 95% CI, −0.011 to −0.001; $P = 0.024$; FDR-corrected $P = 0.041$; adjusted $R^2 = 38.2\%$). After FDR correction, no covariate retained a statistically significant association with the remaining subtypes.

DISCUSSION

Principal Findings

This study characterized Type III popliteal artery variants and their surgical implications via a single-center CTA cohort (235 patients, 470 limbs) and an updated meta-analysis (30 studies, 10,351 limbs). Three findings carry preoperative relevance. First, CTA data confirmed the anatomical commonality of Type III variants and atypical patterns in Chinese patients. Second, morphological analysis demonstrated compensatory peroneal artery enlargement with reversal of the target-artery-to-peroneal-artery diameter ratio from 1.25 (normal) to 0.73 (IIIA) and 0.65 (IIIB). Third, two atypical peri-ankle collateral patterns (1.06% of limbs) featured target-artery hypoplasia with dominant anastomoses rather than diffuse enlargement, easily overlooked on routine CTA. Meta-regression showed CT-based detection was independently associated with lower Type IIIC prevalence ($\beta = -0.108$, FDR-adjusted $P = 0.032$), suggesting the highest-risk variant may be missed by CTA, the modality most used for flap planning. These findings

argue for shifting preoperative assessment from qualitative classification toward quantitative morphometric evaluation and distal perfusion reserve assessment.

Prevalence: Comparison with Global and Regional Data

Our cohort's overall Type III prevalence (6.81%) fell within the wide published range[7, 19, 20]. Type IIIA (3.19%) approximated the global pooled estimate (3.30%) and lay within the East Asian range (2.55–4.12%), consistent with regional PTA deficiency epidemiology. Type IIIB (2.55%) exceeded the global estimate (1.46%) and most individual studies, except Celtikci et al.'s Turkish DSA cohort (5.1%)[21]; 128-slice CTA's higher resolution may detect mild ATA hypoplasia missed by lower-resolution imaging[22]. Type IIIC (peronea arteria magna), the most severe subtype with PA as sole distal inflow, had a global pooled prevalence of 0.56% (range, 0.1–1.66%)[13]; our cohort yielded one limb (0.21%), at the lower spectrum end. Type IIID (PA hypoplasia/aplasia), absent from Kim's 1989 classification but later added[23], had the lowest pooled prevalence (0.13%); our cohort nonetheless identified four cases (0.85%).

Geographic heterogeneity in Type III prevalence was statistically robust and clinically meaningful. South Asia had the highest Type IIIA prevalence (6.56%), whereas East Asia had the lowest (2.55%), a pattern likely attributable to embryonic and genetic influences on arterial development; population-level variation in these processes may underlie the observed geographic differences[24, 25]. Larger, multi-ethnic cohorts with standardized imaging protocols and centralized morphometric assessment are needed to validate geographic variation in Type III popliteal artery variants. CTA studies reported a lower Type IIIC prevalence of 0.34% compared with dissection cohorts. This likely reflects the limited ability of CTA to opacify extremely hypoplastic or thread-like distal vessels in peronea arteria magna, despite its widespread use as a preoperative vascular mapping tool[11]. When tibial arteries were visible on imaging but terminate proximal to the distal foot, Type IIIC variants may be misclassified or entirely overlooked[15]. Because CTA may underestimate the extent of distal tibial artery truncation in Type IIIC, surgeons should maintain a high index of suspicion for this variant, even when CTA reports describe apparently normal tibial anatomy.

Morphometric Reorganization and Its Implications for Flap Surgery

To our knowledge, our morphometric data provide quantitative evidence that Type IIIA and IIIB variants reflect adaptive arterial remodeling, whereas IIID reflects peroneal deficiency with preserved tibial runoff; IIIC was too rare for morphometric inference. In Type IIIA, for example, the PA enlarged to assume the distal perfusion role normally served by the PTA. An inverse correlation between PTA hypoplasia severity and PA enlargement ($r = -0.62$, $P = 0.013$) supported a coordinated, hemodynamically driven response: the more severe the target-artery deficiency, the greater the compensatory PA enlargement. These findings carry direct implications for lower-leg

flap and microsurgical practice, information that cannot be gleaned from branching-pattern classification alone[15]. The affected limb exists in a state of compensated insufficiency. At rest, the enlarged PA maintained adequate distal perfusion, but reduction of independent outflow tracts from three to two, or to one in Type IIIC, necessarily lowers ischemic reserve. When the dominant PA was further compromised, whether by surgical sacrifice during fibular flap harvest, perforator flap dissection, or postoperative thrombosis, the limb may shift from adequate resting perfusion to critical ischemia[26, 27]. Building on these subtype-specific morphometric distinctions, we therefore propose a four-tier perfusion reserve and ischemic risk stratification that integrates anatomical pattern, compensatory mechanism, and flap-specific contraindications to guide preoperative donor-site selection (**Figure 10**).

Given this adaptive remodeling, a normal preoperative vascular examination, including pedal pulse palpation and portable Doppler ultrasonography, neither excludes high-risk Type III variants nor guarantees tolerance of peroneal artery (PA) sacrifice[28]. Karaolanis et al. reported a 76-year-old man with bilateral congenital posterior tibial artery (PTA) aplasia who had palpable pedal pulses and biphasic Doppler signals despite complete PTA absence from the popliteal fossa to the ankle[29]. Similarly, in a consecutive series of 101 fibular flaps, Longo et al. failed to identify a hypoplastic PA (1 mm, terminating 15 cm above the lateral malleolus) on color Doppler; the variant was recognized only intraoperatively[23]. For Type IIIA or IIIB patients considered for free fibular flap, supplementary hemodynamic assessment, such as skin perfusion pressure or intraoperative indocyanine green angiography after temporary PA occlusion, seems prudent before committing to PA sacrifice[30]. Marginal perfusion on these tests warrants serious consideration of an alternative donor site[31]. This recommendation is reinforced by the systematic review of Abou-Foul et al., which demonstrated PA-dependent distal perfusion in 28.4% of limbs across 5,790 cases[10]. Clinical experience further supports this approach. Golas et al. successfully converted a bilateral Type IIIA patient from fibular flap to deep circumflex iliac artery flap after CTA confirmed PA-dependent foot perfusion[31]. Accordingly, we synthesized the available clinical evidence to define actionable risk outcomes associated with Type III popliteal artery variants across all subtypes (**Table 6**), providing a subtype-specific reference for flap selection and donor-site risk stratification.

Preoperative CTA Assessment: A Practical Framework for Microsurgeons

Current preoperative CTA assessment for lower-leg flap surgery is able to display branching-pattern classification and the presence or absence of the three tibial arteries[32]. The present data demonstrate that incorporating morphometric metrics is critical for optimal surgical planning. The multi-dimensional morphometric framework used here, proximal diameters, compensatory vessel terminal diameters, hypoplasia/aplasia classification, termination-point localization, and the target-artery-to-PA diameter ratio,

provides substantially more actionable information for the operating surgeon. A practical CTA report for a flap candidate might include six elements. Branching pattern classification according to Kim-Lippert, with notation of any atypical patterns. Identification of the dominant distal perfusion vessel and its terminal diameter. Classification of any hypoplastic vessel as hypoplasia versus aplasia, with the termination point for aplastic vessels. The target-artery-to-PA diameter ratio as an index of perfusion dominance. An explicit comment on the number of patent vessels at the ankle level. Adopting this standardized reporting would allow microsurgeons to make more informed decisions about flap selection, donor-site risk, and the need for supplementary hemodynamic testing[33].

Based on these elements, we propose a practical framework for microsurgeons to assist surgical decision-making (**Figure 11**). The routine preoperative CTA should be obtained for all patients being considered for lower-leg flap or microsurgical reconstruction. Radiologists should adopt the framework described above rather than relying on branching-pattern classification alone. Surgeons should specifically rule out Type III whenever distal tibial vessels are poorly visualized or when CTA findings are discordant with physical examination.

CONCLUSIONS

This study characterized Type III popliteal artery variants in a Chinese cohort of 235 patients (470 limbs), combined with a meta-analysis of 10,351 limbs. Type III variants affected 6.81% of limbs. In IIIA and IIIB, tibial deficiency was accompanied by PA enlargement and reversed target-artery-to-PA diameter ratios, whereas IIID showed PA deficiency with preserved tibial runoff; IIIC was too rare for morphometric inference. Atypical peri-ankle collateral patterns (1.06%) may be under-recognized on cursory CTA review, and CT-based detection was associated with lower Type IIIC prevalence, possibly reflecting reduced sensitivity for thread-like distal vessels. Standardized multi-dimensional CTA reporting, incorporating diameter ratios and ankle-level vessel patency, is recommended to guide safe lower-leg flap selection.

LIMITATIONS

This study has several limitations. The single-center retrospective design with selection bias limits generalizability. The cohort comprised patients undergoing preoperative CTA for flap planning, a surgically high-risk population that may differ from the general population, and the results were most applicable to this preoperative surgical cohort. Atypical peri-ankle arterial patterns were identified in only 5 limbs. Significant residual heterogeneity and publication bias persisted despite meta-regression and trim-and-fill adjustment. The meta-analysis was not prospectively registered.

Morphometric assessment quantified only anatomical diameters, without concurrent hemodynamic evaluation. Type IIID comprised only 4 limbs.

Abbreviations

ATA: anterior tibial artery; CI: confidence interval; CT: computed tomography; CTA: computed tomography angiography; DSA: digital subtraction angiography; FDR: false discovery rate; ICC: intraclass correlation coefficient; MIP: maximum intensity projection; MRA: magnetic resonance angiography; NOS: Newcastle-Ottawa Scale; PA: peroneal artery; PRISMA: Preferred Reporting Items for Systematic Reviews and Meta-Analyses; PTA: posterior tibial artery; PVM: preoperative vascular mapping; SD: standard deviation.

Declarations

Ethics approval and consent to participate

This study was approved by the Institutional Ethics Committee of the 920th Hospital of Joint Logistic Support Force (approval number 2026-079-1) and was performed in accordance with the Declaration of Helsinki. The requirement for informed consent was waived because of the retrospective nature of the study.

Consent for publication

Not applicable.

Availability of data and materials

Data are available from the corresponding author upon reasonable request. Meta-analysis data are derived from published studies cited in the reference list.

Competing interests

The authors declare no competing interests.

Funding

This work received no specific funding.

Authors' contributions

Xiaoqing He (corresponding author) conceived and designed the study. Yongqing Xu provided clinical expertise and guidance. Yujian Xu and Xi Yang contributed to manuscript drafting and assisted with data processing. Xing Liu performed image data processing and analysis. All authors contributed to the study conception and design and approved the final manuscript.

Acknowledgements

The authors thank the Department of Radiology, 920 Hospital of Joint Logistics Support Force, for technical support in CTA image acquisition and post-processing. We also thank all investigators of the included studies for their published work.

FIGURE LEGENDS

Figure 1. Type III (hypoplasia/aplasia) variants according to Kim and Lippert.

Subtypes IIIA (PTA hypoplasia or aplasia), IIIB (ATA hypoplasia or aplasia), IIIC (combined ATA/PTA hypoplasia or aplasia, peronea arteria magna), and IIID (PA hypoplasia or aplasia). ATA, anterior tibial artery; PTA, posterior tibial artery; PA, peroneal artery.

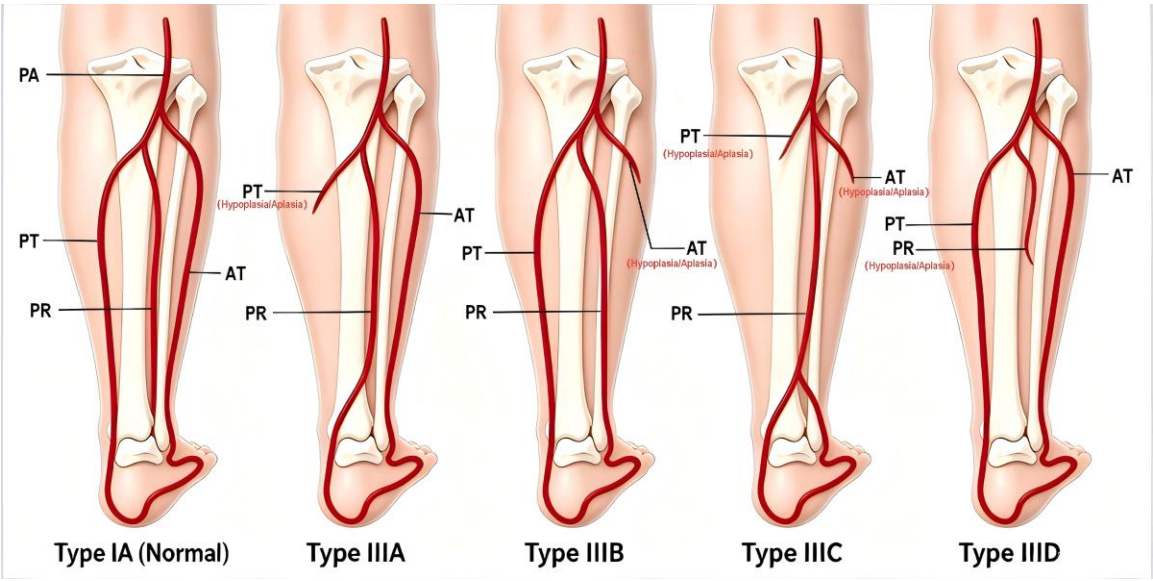


Figure 2. Flowchart of overall study design.

The study integrates a single-center CTA cohort (235 patients, 470 limbs) with a systematic review and meta-analysis (30 studies, 10,351 limbs).

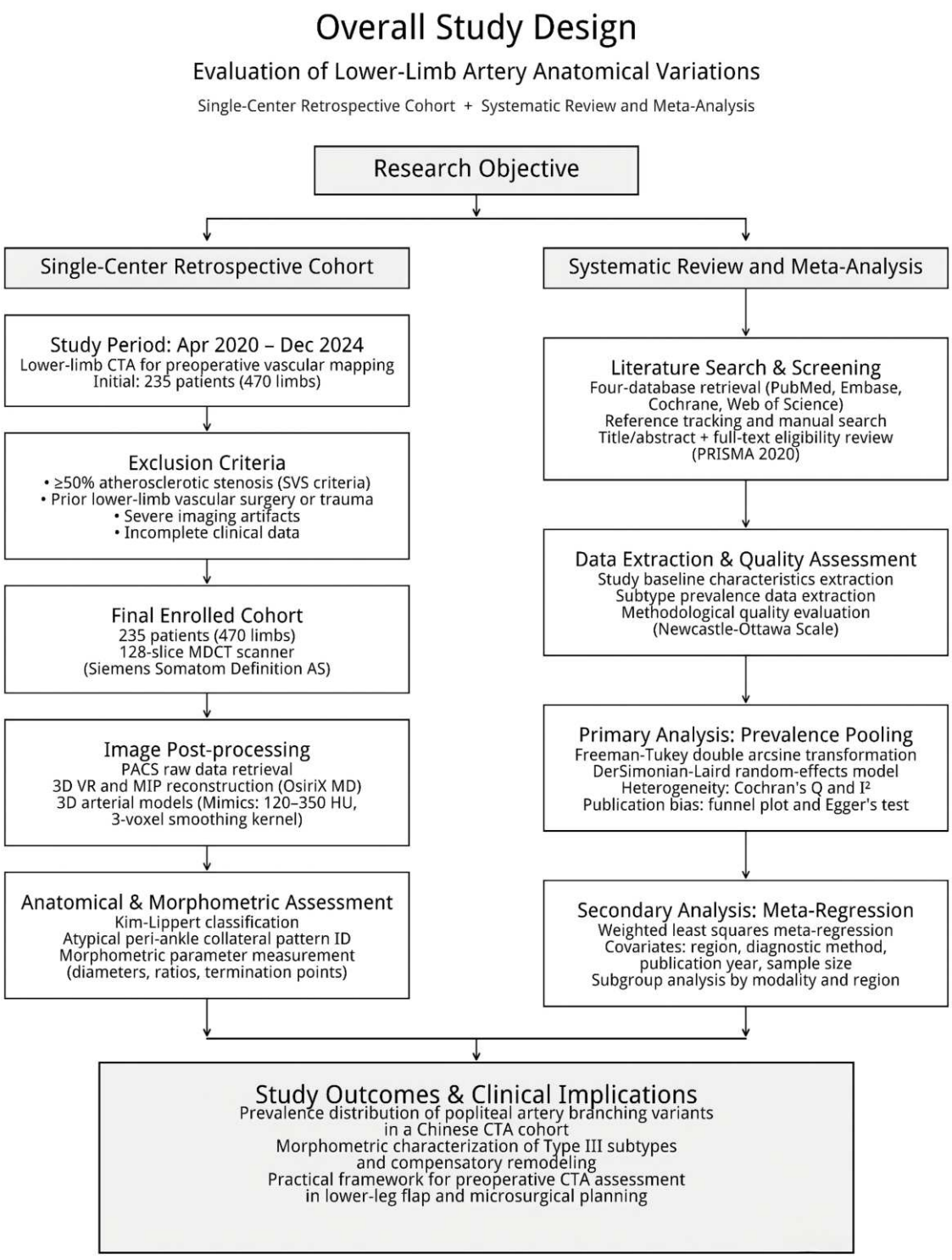


Figure 3. Type IIIA variant: posterior tibial artery (PTA) hypoplasia with compensatory PA enlargement.

(a–c) A 43-year-old woman with a typical unilateral Type IIIA variant in the left lower limb. Axial CT slice (a) shows left PTA absence in the distal lower leg (arrow). Coronal maximum-intensity projection (MIP) reconstruction (b) and three-dimensional volume-rendered image (c) demonstrate PTA attenuation with compensatory enlargement of the peroneal artery (PA) supplying distal perfusion (arrows).

(d–f) A 42-year-old man with a typical bilateral Type IIIA variant. Axial CT slice (d) shows bilateral PTA absence in the distal lower leg (arrows). Coronal MIP reconstruction (e) and three-dimensional volume-rendered image (f) demonstrate bilateral PTA attenuation with compensatory PA enlargement supplying distal perfusion (arrows).

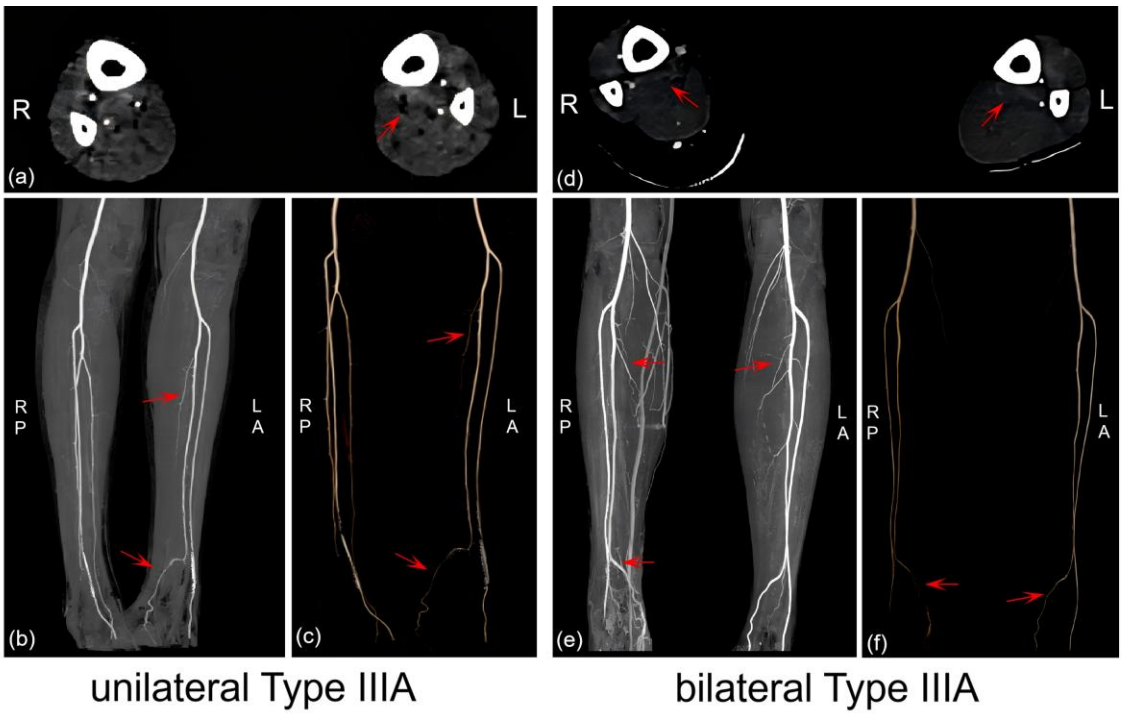


Figure 4. Type IIIB variant: anterior tibial artery (ATA) hypoplasia with peroneal artery (PA) compensation.

(a–c) A 39-year-old man with a typical unilateral Type IIIB variant in the right lower limb. Axial CT slice (a) shows right ATA absence in the distal lower leg (arrow). Coronal maximum-intensity projection (MIP) reconstruction (b) and three-dimensional volume-rendered image (c) demonstrate ATA attenuation with compensatory enlargement of the peroneal artery (PA) supplying distal perfusion (arrows).

(d–f) A 40-year-old man with a typical bilateral Type IIIB variant. Axial CT slice (d) shows bilateral ATA absence in the distal lower leg (arrows). Coronal MIP reconstruction (e) and three-dimensional volume-rendered image (f) demonstrate bilateral ATA attenuation with compensatory PA enlargement supplying distal perfusion (arrows).

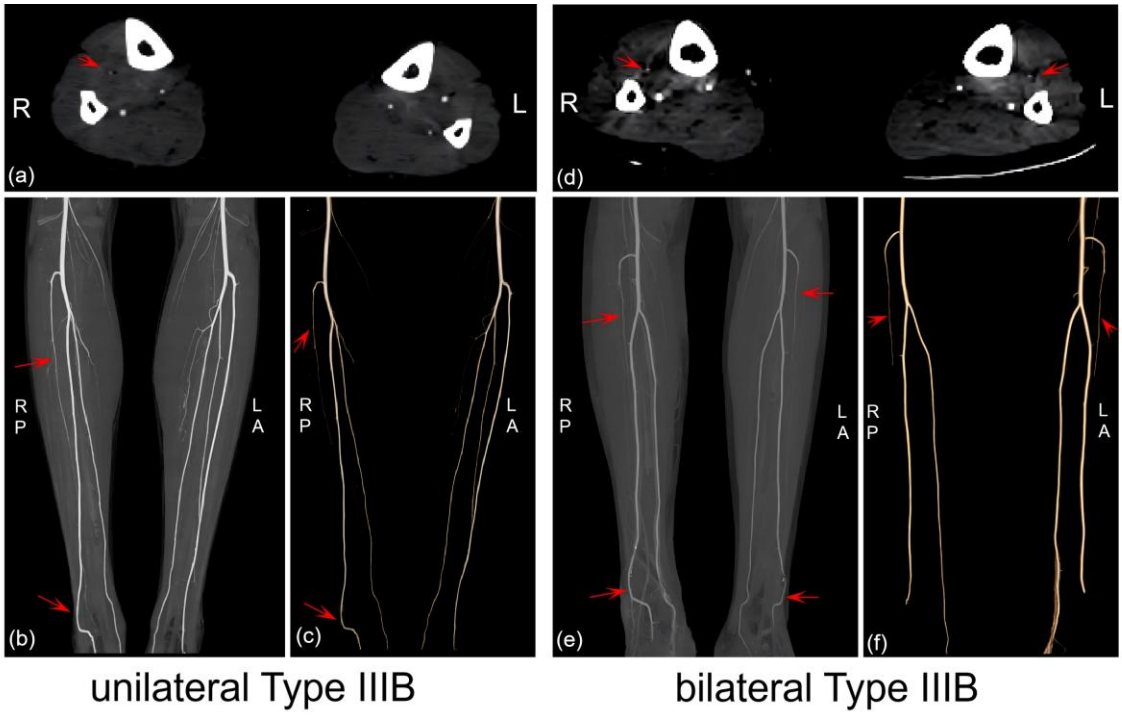


Figure 5. Type IIIC variant (peronea arteria magna): combined ATA and PTA hypoplasia and aplasia.

(a–d) A 44-year-old man with a typical unilateral Type IIIC variant in the left lower limb. Axial CT slice (a) shows absence of the ATA and PTA in the distal lower leg, with the PA as the sole vessel supplying the lower leg and foot (arrows). Coronal maximum-intensity projection (MIP) reconstruction (b) and three-dimensional volume-rendered image (c) demonstrate hypoplasia/aplasia of both the ATA and PTA, with the PA supplying distal perfusion (arrows). Three-dimensional volume-rendered image reconstructed with Mimics software (d) shows PA extension to the distal pedal vessels.

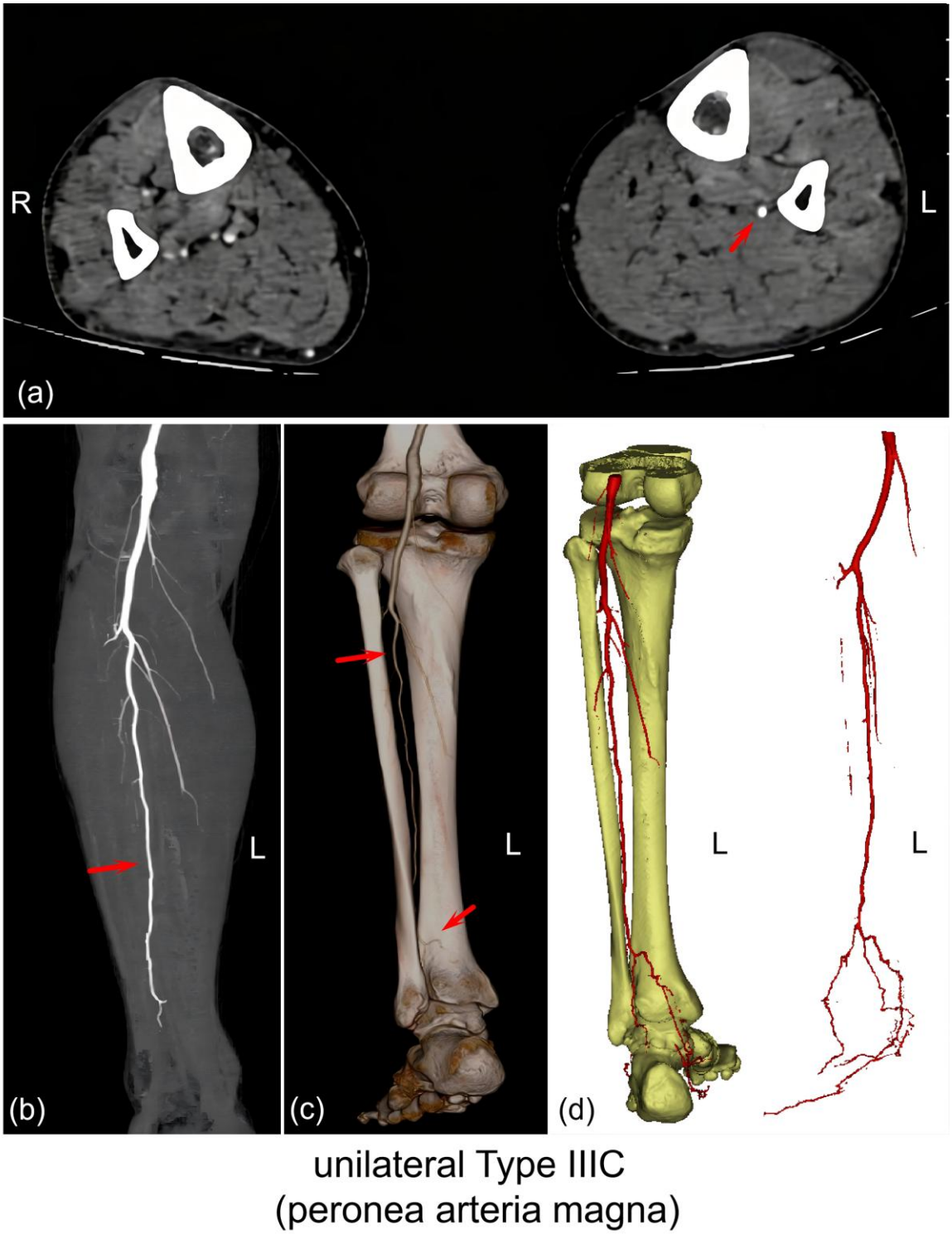


Figure 6. Type IIID variant: peroneal artery (PA) hypoplasia with preserved tibial arteries.

(a–c) A 49-year-old woman with a typical unilateral Type IIID variant in the right lower limb. Axial CT slice (a) shows right PA hypoplasia in the distal lower leg (arrow).

Coronal maximum-intensity projection (MIP) reconstruction (b) and three-dimensional volume-rendered image (c) demonstrate the right PA attenuation and absence in the distal lower leg while the PTA and ATA maintain normal distal perfusion (arrows).

(d–f) A 43-year-old man with a typical bilateral Type IIID variant. Axial CT slice (d) shows bilateral PA absence in the distal lower leg (arrows). Coronal MIP reconstruction (e) and three-dimensional volume-rendered image (f) demonstrate the bilateral PA attenuation and absence in the distal lower leg while the PTA and ATA maintain normal distal perfusion (arrows).

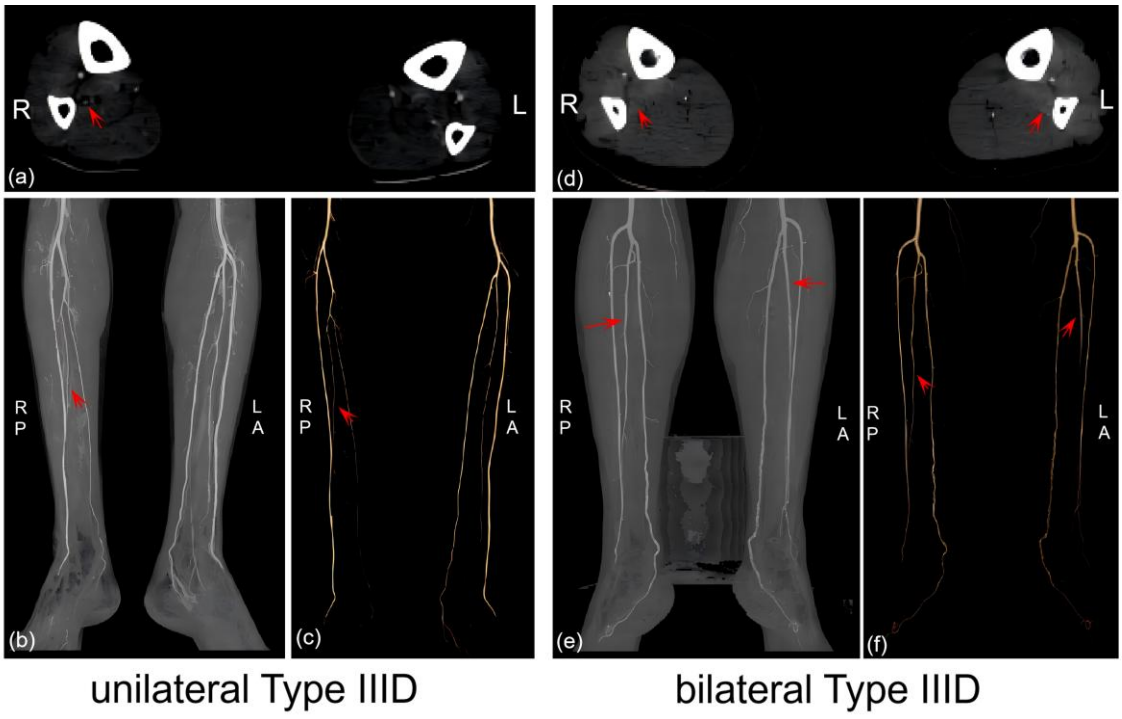


Figure 7. Atypical peri-ankle collateral-dominant pattern: hypoplastic target artery with ankle anastomoses.

(a–d) A 72-year-old woman with an atypical peri-ankle collateral-dominant pattern in the right lower limb. Axial CT slice (a) shows that thick side branches anastomose between the PA and PTA at the ankle joint (arrow). Coronal maximum-intensity projection (MIP) reconstruction (b) and three-dimensional volume-rendered image (c) demonstrate hypoplasia of the ATA with robust collateral anastomoses between PA and PTA at the ankle joint (arrows). Three-dimensional volume-rendered image reconstructed with Mimics software (d) provides an overview of the lower extremity vasculature.

(e–h) A 27-year-old man with bilateral atypical peri-ankle collateral-dominant pattern. Axial CT slice (e) shows that bilateral branches anastomose between the peroneal and posterior tibial arteries at the ankle joint (arrow). Coronal maximum-intensity projection

(MIP) reconstruction (f) and three-dimensional volume-rendered image (g) demonstrate that the bilateral PTAs are hypoplastic but remain intact, and robust collateral anastomoses between the PA and PTA at the ankle joint (arrows). Three-dimensional volume-rendered image reconstructed with Mimics software (h) provides an overview of the lower extremity vasculature.

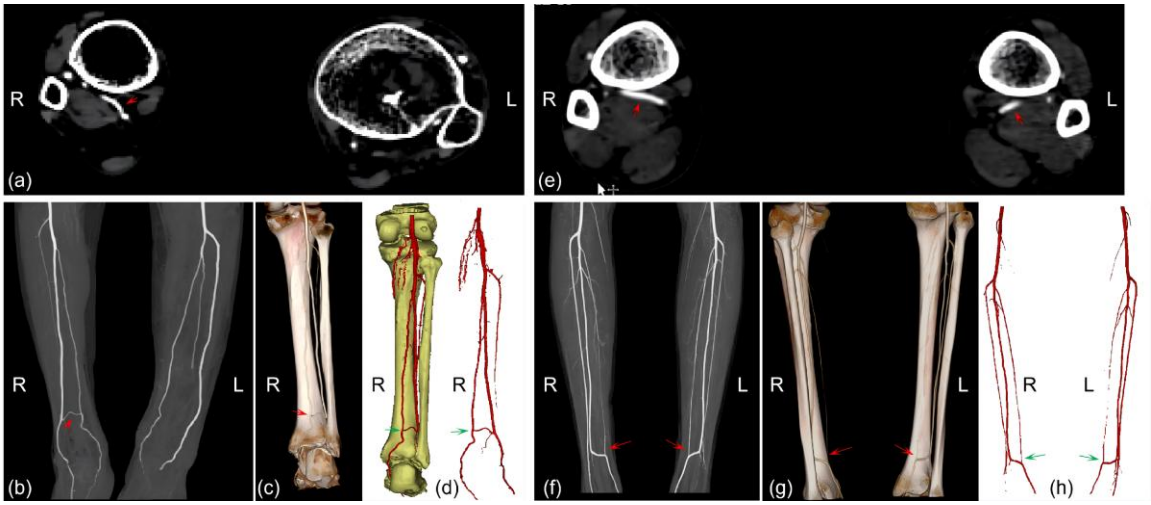
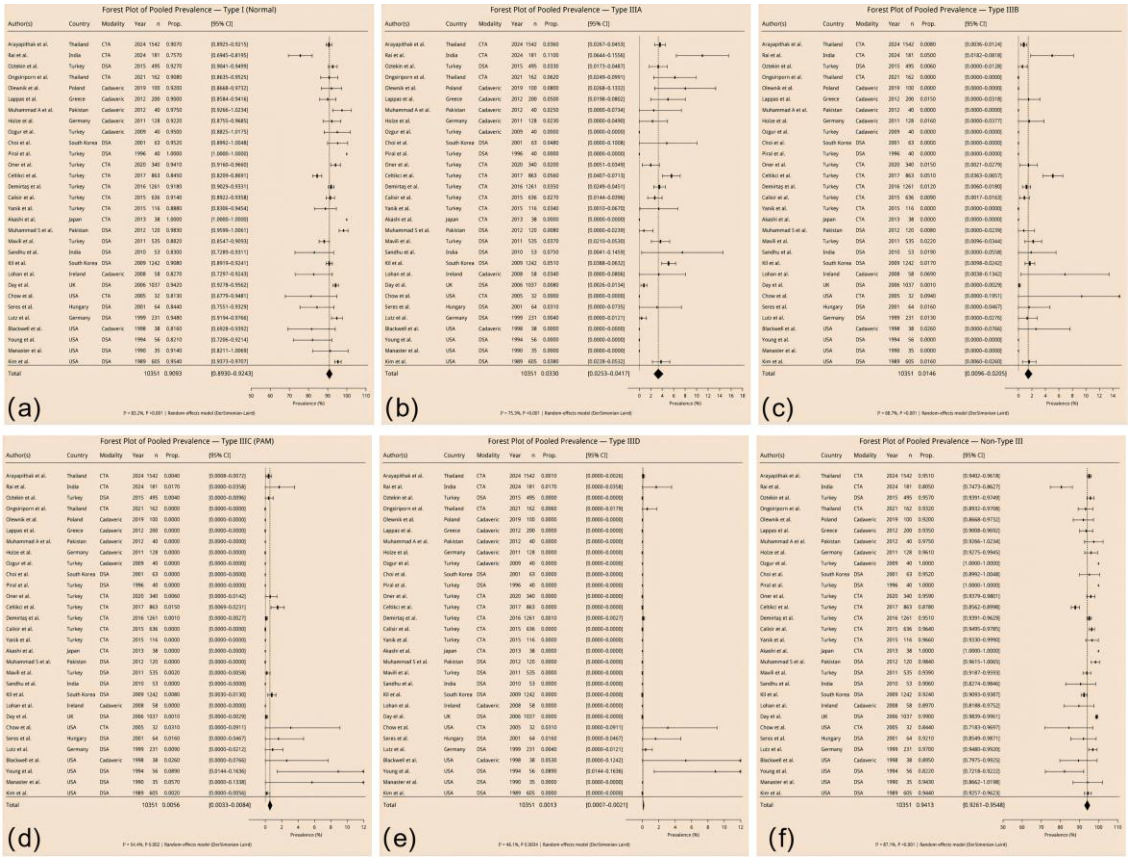


Figure 8. Forest plots of pooled prevalence estimates for popliteal artery branching patterns in the meta-analysis.

Random-effects meta-analysis (DerSimonian-Laird model with Freeman-Tukey double arcsine transformation) of 30 studies comprising 10,351 lower extremities. Forest plots are shown for (a) Type I (normal), (b) Type IIIA, (c) Type IIIB, (d) Type IIIC (peronea arteria magna), (e) Type IIID, and (f) non-Type III patterns.



527

528 **Figure 9. Subgroup analysis of pooled prevalence by diagnostic modality and**
529 **geographic region.**

530 Bar charts comparing pooled prevalence estimates across prespecified subgroups. (a)
531 Type I and Type III prevalence by diagnostic method (angiography, CT-angiography,
532 anatomical dissection). (b) Type III subtype prevalence (IIIA, IIIB, IIIC, IIID) by
533 diagnostic method. (c) Type I and Type III prevalence by geographic region (North
534 America, East Asia, Europe, West Asia, South Asia). (d) Type III subtype prevalence by
535 geographic region.

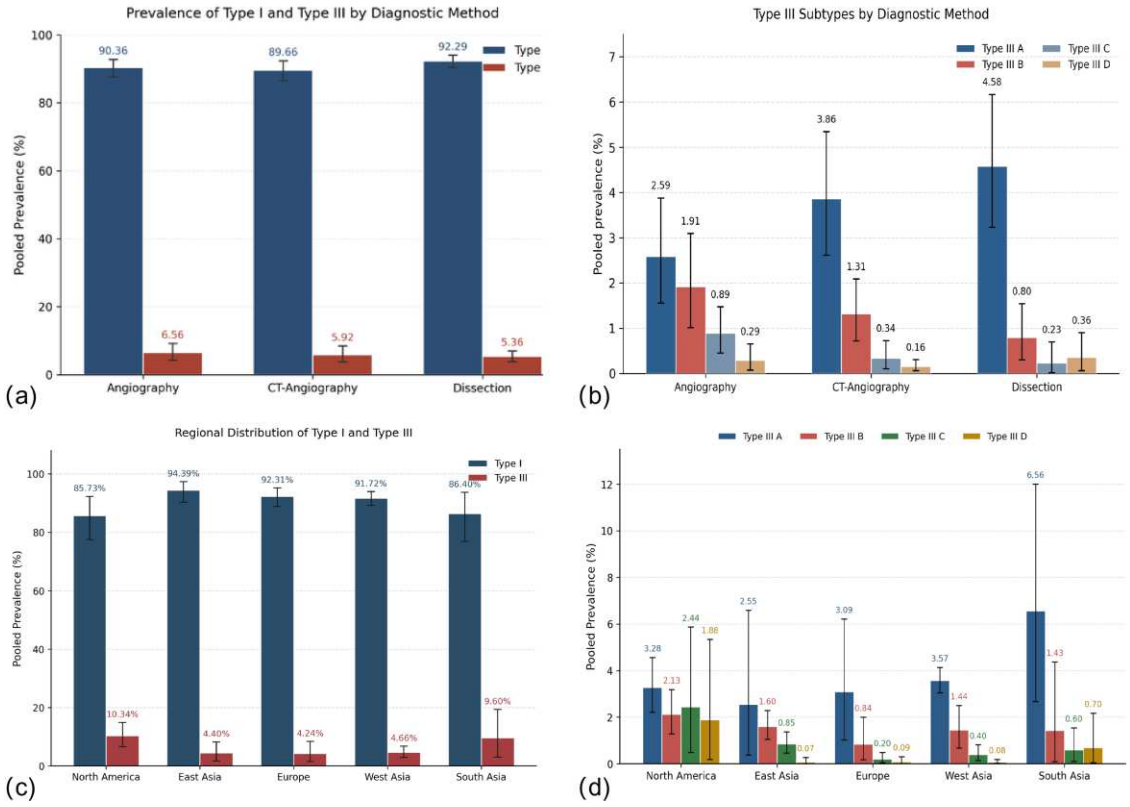


Figure 10. Anatomy-derived perfusion reserve and theoretical ischemic risk stratification of Type III popliteal artery variants for lower-leg flap surgery.

Four-tier grading system mapping anatomic subtypes to surgical risk. Grade I (adequate reserve, low risk): Type IIID — ATA and PTA preserved with isolated PA deficiency; limb perfusion maintained, but PA-based flaps are unsuitable due to a deficient pedicle. Grade II (compensated reserve, moderate risk): Atypical peri-ankle collateral patterns — target-artery hypoplasia offset by prominent ankle anastomoses preserving pedal arch integrity; flap selection requires collateral adequacy assessment. Grade III (insufficient reserve, high risk): Type IIIA and IIIB — tibial artery deficiency with PA compensation; PA sacrifice risks distal ischemia, and free fibular flap is a relative contraindication. Grade IV (absent reserve, absolute contraindication): Type IIIC (peronea arteria magna) — PA is the sole distal feeder; any PA sacrifice is absolutely contraindicated.

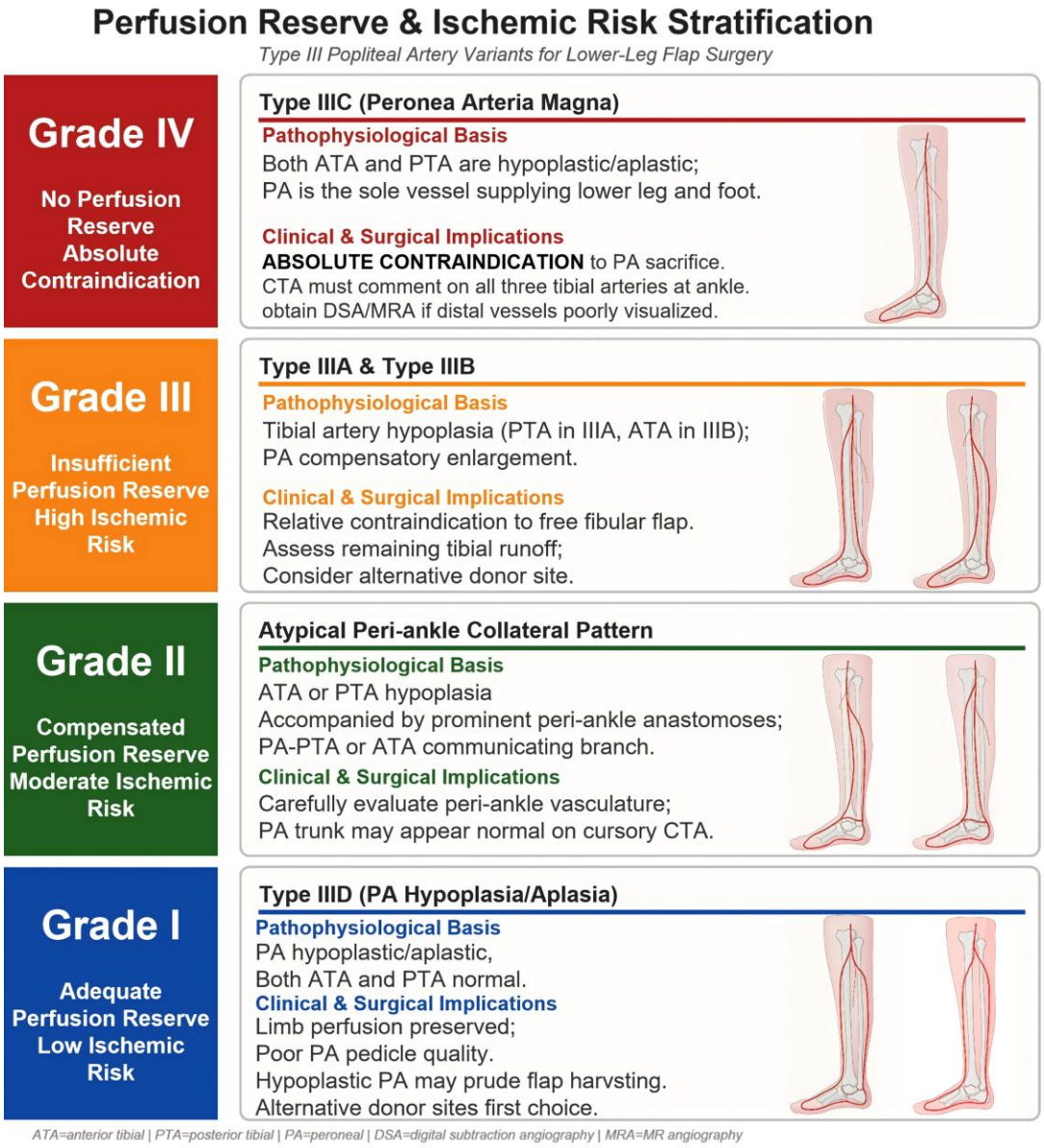
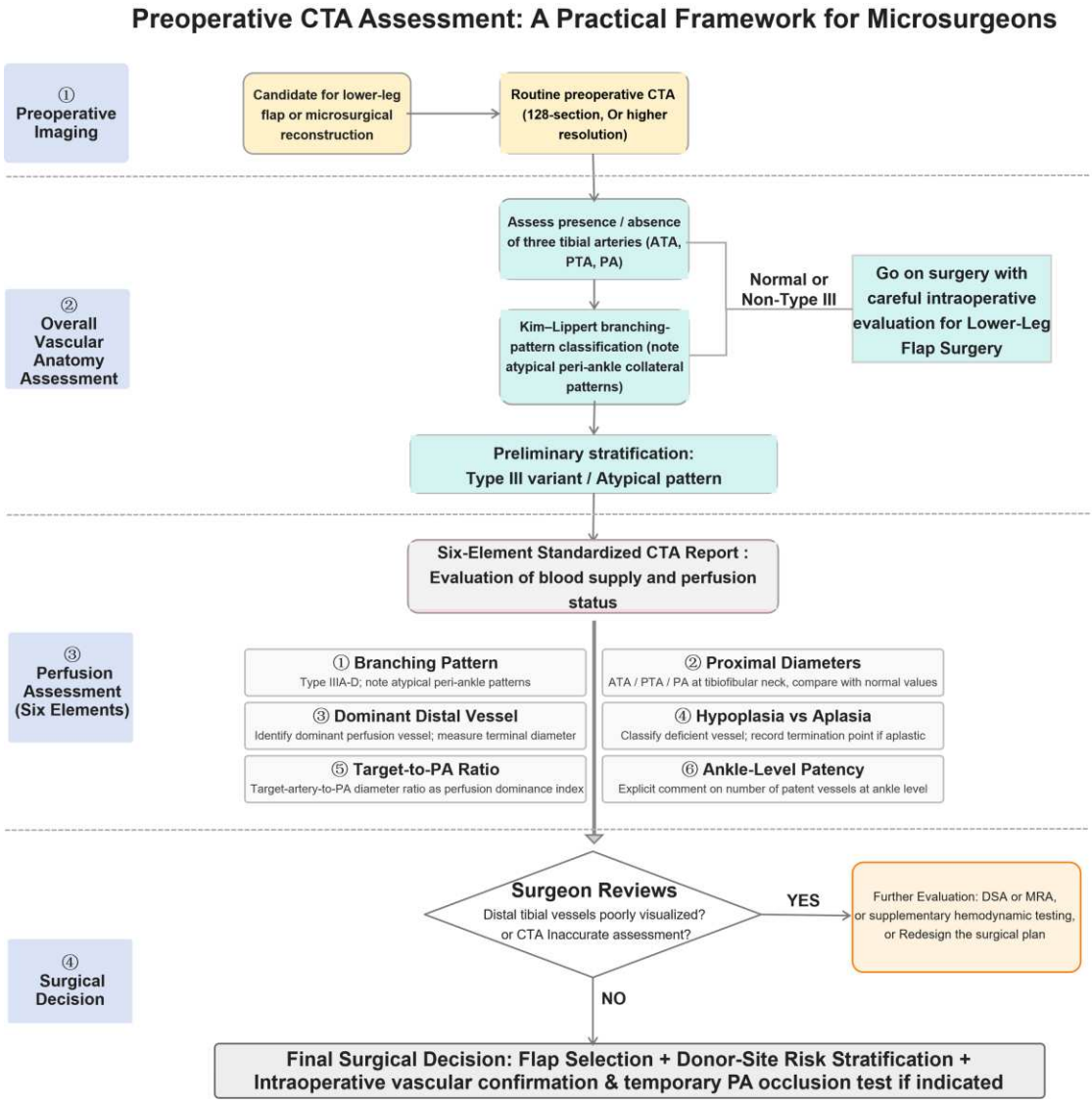


Figure 11. Practical framework for preoperative CTA assessment in lower-leg flap and microsurgical reconstruction.

Four-stage clinical decision pathway. Stage 1 (Preoperative Imaging): routine CTA for all flap candidates. Stage 2 (Anatomical Assessment): evaluate ATA, PTA, and PA patency; classify per Kim-Lippert, noting atypical peri-ankle collaterals. Non-Type III limbs proceed to surgery. Stage 3 (Perfusion Assessment): standardized report including (1) branching pattern, (2) proximal diameters, (3) dominant distal vessel and terminal diameter, (4) hypoplasia/aplasia with termination point, (5) target-artery-to-PA ratio, (6) ankle-level patency. Stage 4 (Surgical Decision): further imaging (DSA/MRA) or hemodynamic testing if distal vessels are poorly visualized; final flap selection, donor-site risk stratification, and intraoperative PA occlusion test when indicated.



Supplementary Figure 1. PRISMA 2020 flowchart of study selection for the systematic review and meta-analysis.

Supplementary Figure 2. Forest plots and funnel plots for each Type III subtype in the meta-analysis.

References

[1] Kil SW, Jung GS. Anatomical variations of the popliteal artery and its tibial branches: analysis in 1242 extremities. Cardiovasc Intervent Radiol. 2009;32:233-240.

[2] Miao Z, Chen C, Qiu Q, Wu C. Ultrasound in diagnosis of anatomical variation of anterior and posterior tibial arteries. Med Ultrason. 2016;18:64-69.

[3] Astarci P, Siciliano S, Verhelst R, et al. Intra-operative acute leg ischaemia after free fibula flap harvest for mandible reconstruction. Acta Chir Belg. 2006;106:423-426.

[4] May H, Kastan O, Emre TY, Cetin M, Unal M, Kose O. Anterior Tibial Artery and Its Clinical Importance in the Posterolateral Approach to the Tibial Plateau: An Angiographic Study on 219 Lower Limbs. J Knee Surg. 2022;35:725-730.

[5] Lippert H, Pabst R. Arterial Variations in Man: Classification and Frequency. 1985. Munich. J. F. Bergmann Verlag. 121.

[6] Kim D, Orron DE, Skillman JJ. Surgical significance of popliteal arterial variants. A unified angiographic classification. Ann Surg. 1989;210:776-781.

[7] Oner S, Oner Z. Popliteal Artery Branching Variations: A Study on Multidetector CT Angiography. Sci Rep. 2020;10:8147.

[8] Vazquez T, Rodríguez-Niedenfuhr M, Parkin I, Viejo F, Sanudo J. Anatomic study of blood supply of the dorsum of the foot and ankle. Arthroscopy. 2006;22:287-290.

[9] Bellezza PA, Elliott E, Conlee T, Clements JR. Aplastic Posterior Tibial Artery in the Presence of Trimalleolar Ankle Fracture Dislocation Resulting in Below-the-Knee Amputation. J Foot Ankle Surg. 2017;56:92-97.

[10] Abou-Foul AK, Borumandi F. Anatomical variants of lower limb vasculature and implications for free fibula flap: Systematic review and critical analysis. Microsurgery. 2016;36:165-172.

[11] Ma C, Wang L, Tian Z, et al. Standardize routine angiography assessment of leg vasculatures before fibular flap harvest: lessons of congenital and acquired vascular anomalies undetected by color Doppler and physical examinations. Acta Radiol. 2021;62:1716-1725.

[12] Gürlek Çelik N, Fazlıoğulları Z, Karabulut AK, Nayman A. Variations in the branching pattern of the popliteal artery: a CT angiography study. Anatomy. 2021;15:216-222.

[13] Rai A, Chopra J, Irfan A, et al. Variations in the Termination of the Popliteal Artery: A Multidetector Computed Tomography Angiography (CTA)-Based Retrospective Study. Cureus. 2024;16:e63092.

[14] Aragonés P, Rodríguez-Niedenführ M, Quinones S, et al. Popliteal artery: Anatomical study and review of the literature. Ann Anat. 2021;234:151654.

[15] Abou-Foul AK, Fasanmade A, Prabhu S, Borumandi F. Anatomy of the vasculature of the lower leg and harvest of a fibular flap: a systematic review. Br J Oral Maxillofac Surg. 2017;55:904-910.

[16] Ahn L, Christensen JM, Fruge S, Meulendijks MZ, Hoftiezer YAJ, Wong FK, et al. Preoperative vascular imaging in lower extremity free flap reconstruction: comparison between imaging modalities. Microsurgery. 2024;44:e31241.

[17] Knitschke M, Baumgart AK, Bäcker C, Adelung C, Roller F, Schmermund D, et al. Computed tomography angiography (CTA) before reconstructive jaw surgery using fibula free flap: retrospective analysis of vascular architecture. Diagnostics. 2021;11:1865.

[18] Page MJ, McKenzie JE, Bossuyt PM, et al. The PRISMA 2020 statement: an updated guideline for reporting systematic reviews. BMJ. 2021;372:n71.

[19] Tomaszewski KA, Popieluszko P, Graves MJ, et al. The evidence-based surgical anatomy of the popliteal artery and the variations in its branching patterns. J Vasc Surg. 2017;65:521-529.e6.

[20] Arayapithak K, Suwannanon R, Hongsakul K. Popliteal artery branching variations on computed tomography angiography of 1542 lower limbs and its associated factors. Acta Radiol. 2023;64:874-880.

[21] Celtikci B, Ozturk MK, Adibelli G, et al. Evaluation of popliteal artery branching variations with digital subtraction angiography. Diagn Interv Radiol. 2017;23:227-232.

[22] Demirtaş H, Değirmenci B, Çelik AO, et al. Anatomic variations of popliteal artery: Evaluation with 128-section CT-angiography in 1261 lower limbs. Diagn Interv Imaging. 2016;97:635-642.

[23] Longo B, Sorotos M, Nicolotti M, Santanelli di Pompeo F. Retrospective analysis of incidence of peroneal artery hypoplasia in 101 free fibula transfers and new classification of popliteal branch anomalies. Injury. 2014;45:394-398.

[24] Mauro MA, Altman RD, Trerotola SO, et al. Popliteal artery branching: embryologic and angiographic correlation. Radiology. 1988;166:761-765.

[25] Kuznetsov AV, Shchelkunov AN, Bykanov AN, et al. Popliteal artery anatomy: a comprehensive review with clinical and surgical correlations. Folia Morphol. 2023;82:543-556.

[26] Knitschke M, Baumgart AK, Bäcker C, et al. Impact of Periosteal Branches and Septo-Cutaneous Perforators on Free Fibula Flap Outcome: A Retrospective Analysis of Computed Tomography Angiography Scans in Virtual Surgical Planning. Front Oncol. 2021;11:821851.

[27] Linderson A, Dimovska EOF, Rodriguez-Lorenzo A. Donor site ischemic events following fibula flap harvest in head and neck reconstruction: a case report and perioperative management strategies. Int Microsurg J. 2022;6:1.

[28] Alolabi N, Augustine H, Farrokhyar F, Levis C. Preoperative Angiography for Free Fibula Flap Harvest: A Case Series. Plast Surg (Oakv). 2022;30:108-112.

[29] Karaolanis G, Galyfos G, Karanikola E, Palla VV, Filis K. Absence of Clinical and Hemodynamic Consequences due to Posterior Tibial Artery Congenital Aplasia. Case Rep Vasc Med. 2015;2015:821094.

[30] Ludolph I, Horch RE, Arkudas A, Schmitz M. Enhancing Safety in Reconstructive Microsurgery Using Intraoperative Indocyanine Green Angiography. Front Surg. 2019;6:39.

[31] Golas MM, Cray JJ, Huamani JP. An algorithm for the use of CT angiography in planning free fibula flap harvest. J Craniofac Surg. 2016;27:455-459.

[32] Ono S, Ohi H, Ogawa R. Imaging in Propeller Flap Surgery. Semin Plast Surg. 2020;34:145-151.

[33] Lange CJ, Thimmappa ND, Boddu SR, et al. Automating Perforator Flap MRA and CTA Reporting. J Digit Imaging. 2017;30:350-357.

Supplementary Files

This is a list of supplementary files associated with this preprint. Click to download.

- Table1BaselineCharacteristics.docx
- Table2PrevalenceandLaterality.docx
- Table3MorphometricAssessment.docx
- Table4PooledPrevalence.docx
- Table5MultivariableMetaRegression.docx
- Table6ClinicalImplicationsforFlapSurgeryandMicrosurgicalPlanning.docx
- SupplementaryTable1CTAImagingProtocol.docx
- SupplementaryTable2SystematicSearchStrategy.docx
- SupplementaryTable3IncludedStudiesCharacteristics.docx
- SupplementaryTable4SubgroupAnalysisResults.docx
- SupplementaryFigure1.tif
- SupplementaryFigure2.tif